Hot Rolling and Quench Rolling of Ultrahigh Molecular Weight Polyethylene

AKIRA KAITO, KAZUO NAKAYAMA, and HISAAKI KANETSUNA,
Research Institute for Polymers and Textiles, 1-1-4, Yatabe-Higashi Tsukuba, Ibaraki 305, Japan

Synopsis

The mechanical properties, the crystal orientation, and the microstructure of hot rolled and quench rolled ultrahigh molecular weight polyethylene (UHMW-PE) were investigated. The tensile strength of hot rolled and quench rolled UHMW-PE sheets increased with increasing draw ratio. The crystallographic axes a, b, and c of the rolled sheets tended to be oriented to the normal direction (ND), the traverse direction (TD), and the rolling direction (RD), respectively. The small-angle X-ray scattering patterns with incident X-ray beam parallel to TD suggested the presence of inclined lamellar structure in the RD–ND plane. At the initial stage of rolling, partial breakup of crystallites along the (100) plane was observed. The lamellar structure is deformed by the slippage mechanism along the (100) plane in the chain direction.

INTRODUCTION

The rolling of polymeric materials is one of the helpful methods for modifying mechanical properties of polymers. The tensile strength of polymers in the rolling direction was shown to increase by rolling.[1,2] The structural changes of polymeric materials caused by rolling was extensively studied. The orientation of crystallographic axes of rolled polymers was clarified by the measurements of wide angle X-ray diffraction (WAXD).[2–7] The deformation of lamellar structure by rolling was investigated by small angle X-ray scattering (SAXS).[2,4,6,8]

Kwei et al. examined quench rolling of polyethylene (PE).[9,10] They crystallized the PE melt by high speed quenching between a pair of rollers which were rotating at high shear rate. The mechanical and thermal properties of the quench rolled film was investigated.[10]

On the other hand, ultrahigh molecular weight polyethylene (UHMW-PE) is noted as a polymer with excellent physical and mechanical properties, such as high toughness, abrasion resistance, low coefficient of friction, and corrosion resistance to the attack of chemicals.[11,12] Meinel and Peterlin studied the mechanical properties and morphology of cold rolled UHMW-PE.[13] Recently Han et al. reported the cold rolling of powder processed UHMW-PE.[14] However, details in the microstructure of hot rolled UHMW-PE have not been reported.

This work was undertaken on the hot rolling and quench rolling of UHMW-PE, in order to elucidate the mechanical properties, crystal orientation, and microstructure of rolled UHMW-PE.

Journal of Applied Polymer Science, Vol. 28, 1207–1220 (1983)
 CCC 0021-8995/83/031207-14$02.40

TABLE I
UHMW-PE Used in This Work

Grade	$\overline{M}_v$[a]	T_m[a,b] (°C)	T_{mp}[c] (°C)
Hizex Million 145 M	700,000		131.6
Hizex Million 240 M	1,900,000	136	131.1
Hizex Million 340 M	2,700,000	136	132.0

[a] Supplier's data.
[b] T_m = melting temperature determined by the visual observation under a polarizing microscope.
[c] T_{mp} = peak melting temperature on the DSC curve.

EXPERIMENTAL

Sample Preparation

The samples used in this work were three grades of UHMW-PE, Hizex Million (Mitsui Petrochemical Co., Ltd.), whose molecular weights and melting points are summarized in Table I. The sheets 0.9–1.1 mm thick were obtained by compression moulding the powder of UHMW-PE at 220–250°C under a pressure of 6–7 MPa. The sheet was cut into strips 10 mm wide, which were used for the experiment.

Preheating and rolling temperatures are summarized in Table II. The UHMW-PE sheets were preheated to the same temperature as rollers and succeedingly rolled using a pair of heated rollers with a diameter of 50 mm (hot rolling). In addition to the hot rolling at constant temperature, we carried out the crystallization from the melt under rolling (quench rolling). Molten UHMW-PE sheets were rolled and crystallized with passing through a pair of rollers whose temperature was set below melting temperature of the UHMW-PE sheet. Turning speed of rollers was set to be 1 m/min.

Characterization

Tensile properties were measured at 23 ± 1°C and a relative humidity of 50 ± 2% on a tensile testing machine, Tensilon UTM-III-100 (Toyo Baldwin Co., Ltd.), using a 16-mm gauge length and at a 4 mm/min tensile rate. Young's modulus was determined from the slope of the stress–strain curve within 1% strain.

WAXD patterns were obtained with Ni-filtered CuKα radiation (40 kV, 25

TABLE II
Preheating and Rolling Temperatures

	Preheating temp (°C)	Rolling temp (°C)
Hot rolling	70–130 (below T_m)	70–130 (below T_m)
Quench rolling	150 (above T_m)	70–120 (below T_m)

mA) produced by a Geiger Flex XGC-20 (Rigaku Denki Co., Ltd.). WAXD scanning was carried out using a scintillation counter together with a pulse height analyzer.

In order to clarify orientation of the a- and b-axes, 200 and 020 pole figures were obtained by employing both reflection and transmission techniques. The X-ray intensity was corrected for background and absorption.

The crystallite sizes were calculated from the integrated line width using a Scherrer equation,[15] after the WAXD intensity profiles were corrected for instrumental and Kα doublet broadenings.

SAXS patterns were taken with a vacuum camera. Ni-filtered CuKα radiation (40 kV, 100 mA) produced by a Rota Flex RU-200 (Rigaku Denki Co., Ltd.) and pinhole collimators with 0.2–0.5-mm diameter were used. In order to evaluate the periodicity, the SAXS intensity distribution was measured using a scintillation counter.

The melting behavior of the samples was examined at a constant heating rate of 5°C/min with a Perkin-Elmer DSC-2 Differential Scanning Calorimeter. The temperature was calibrated with standard samples of Indium (T_m = 156.5°C) and benzil (T_m = 95°C).

Density was measured using a ethanol–water density gradient column at 25°C. The degree of crystallinity, the weight fraction of the crystalline phase, was calculated assuming the two-phase model. The densities of the crystalline and amorphous phases were taken to be 0.999 g/cm^3 and 0.8525 g/cm^3, respectively.[16,17]

RESULTS

Appearance

By hot rolling and quench rolling the UHMW-PE sheets became transparent. The thickness of the sheets elastically recovered in part after they had passed through rollers. The degree of thickness recovery increased with increasing rolling temperature, T_r. There was a small, but measurable expansion of width by hot rolling and quench rolling. Here, the draw ratio λ was defined by the ratio of length before and after rolling.

Effect of Molecular Weight and Rolling Temperature on the Maximum Draw Ratio

As shown in Figure 1, the maximum draw ratio λ_{max} decreased with increasing molecular weight, for both hot rolling and quench rolling. The value of λ_{max} obtained by hot rolling was higher at T_r = 100°C [Fig. 1(a)]. In the case of quench rolling, the highest draw ratio was achieved at T_r = 100°C or 120°C [Fig. 1(b)].

Tensile Properties

Hot rolled and quench rolled UHMW-PE were uniformly deformed without necking during tensile test. The tensile properties versus draw ratio for 240 M sheets are shown in Figure 2. With increasing draw ratio, the tensile strength

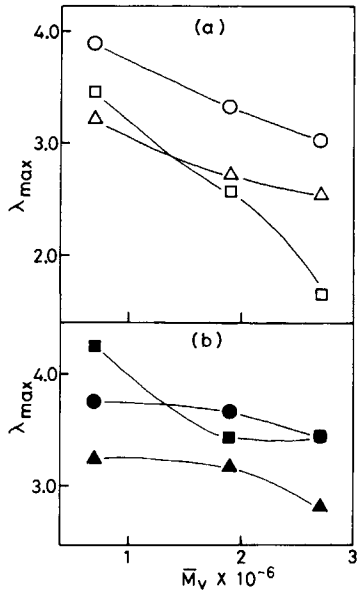

Fig. 1. Maximum draw ratio (λ_{max}) vs. molecular weight relationship. (a) Hot rolled sheet: (△) rolling temperature; T_r = 70°C; (○) T_r = 100°C; (□) T_r = 130°C. (b) Quench rolled sheet: (▲) T_r = 70°C; (●) T_r = 100°C; (■) T_r = 120°C.

increased and the strain at break decreased. In the case of hot rolled sheets, the Young's modulus was less varied with draw ratio in the low draw ratio range ($\lambda < 2.6$), but slightly increased at a higher draw ratio. On the other hand, the

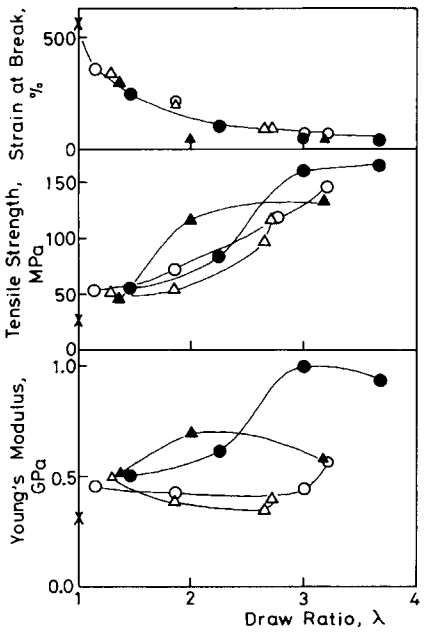

Fig. 2. Tensile properties vs. draw ratio (λ) relationship for 240 M sheets: (△) hot rolled sheet, T_r = 70°C; (○) hot rolled sheet, T_r = 100°C; (▲) quench rolled sheet, T_r = 70°C; (●) quench rolled sheet, T_r = 100°C.

Young's modulus of the quench rolled sheet increased with draw ratio in the low draw ratio range, and slightly decreased at a higher draw ratio.

Crystal Orientation

The 200 and 020 pole figures measured for the hot rolled 240 M sheets are given in Figures 3–5. The principal axes of the rolled sheet are labeled RD (rolling direction), TD (traverse direction), and ND (normal direction to the sheet plane). The contour lines were drawn in units of the intensity of a random sample. In the lightly rolled sample ($\lambda = 1.14$), the 200 pole maximum lay at ND and the 020 pole was distributed in all direction with maximum at TD (Fig. 3). At the

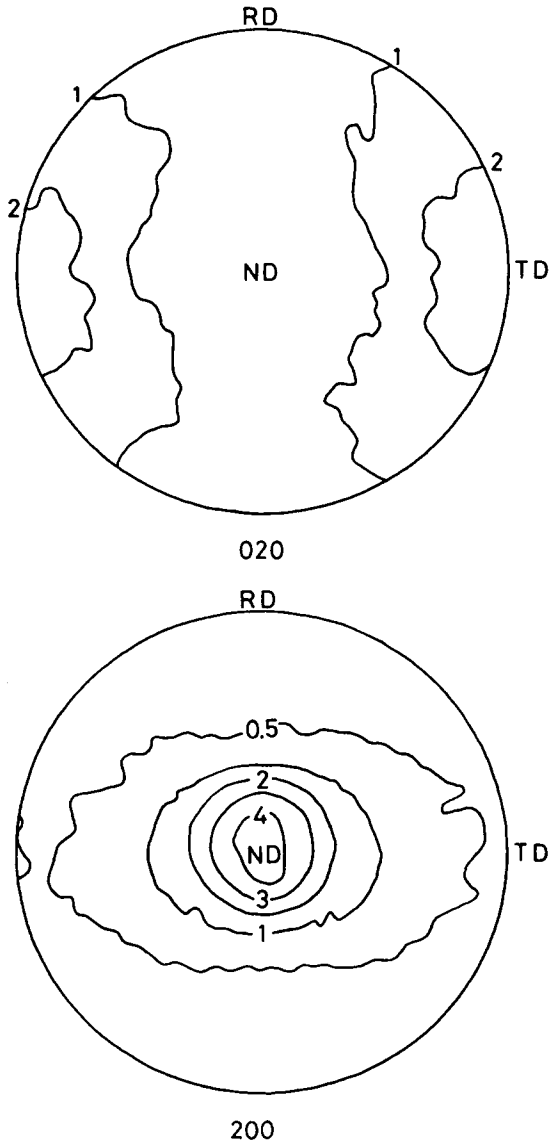

Fig. 3. WAXD pole figures of the hot rolled 240 M sheet ($T_r = 100°C$, $\lambda = 1.14$).

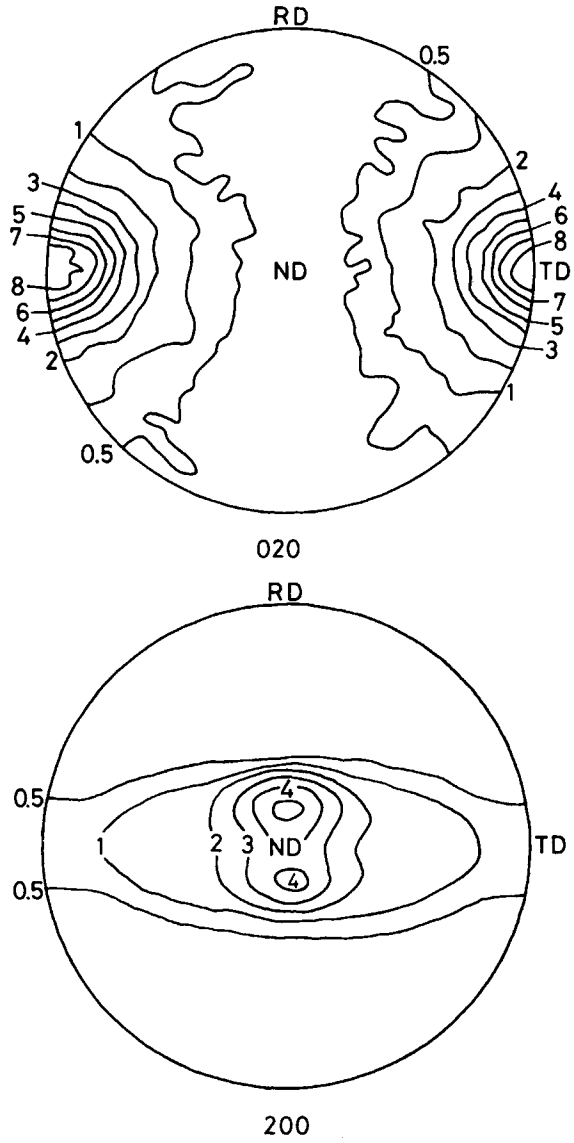

Fig. 4. WAXD pole figures of the hot rolled 240 M sheet (T_r = 100°C, λ = 1.86).

middle stage of rolling (λ = 1.86), the 200 pole maximum lay in the RD–ND plane at an angle of 15° from ND (Fig. 4). The 020 pole became sharply distributed to TD at this stage (Fig. 4). This implies that the c-axis was tilted from RD in the RD–ND plane. In the heavily rolled sample (λ = 3.33), the 200 pole was concentrated on the ND–TD line and had two maxima, the higher one at ND and the other much lower at 57° from ND (Fig. 5). The 020 pole was also located on the ND–TD line with higher maximum at TD and lower maximum at 59° from TD (Fig. 5).

The 200 and 020 pole figures of the quench rolled sheet with λ = 1.48 are presented in Figure 6. The 200 pole was distributed in both RD–ND and

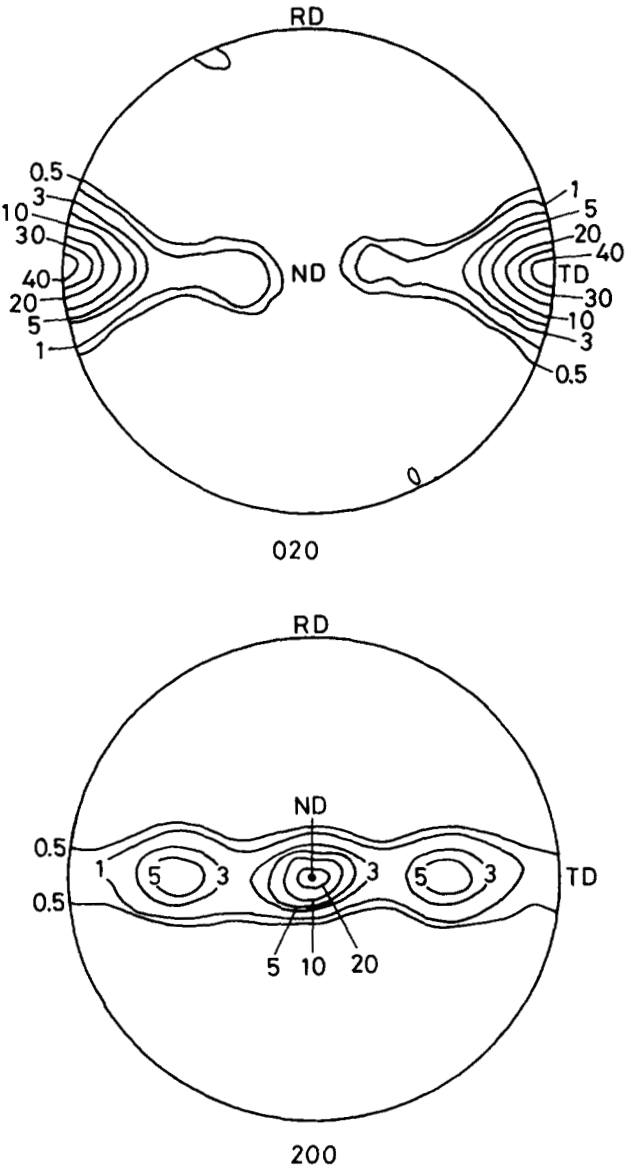

Fig. 5. WAXD pole figures of the hot rolled 240 M sheet (T_r = 100°C, λ = 3.33).

ND–TD lines. The 200 and 020 pole maxima were observed on ND and TD, respectively, similarly to the lightly hot rolled sheet (Fig. 3). As the *b*-axis is the axis of crystal growth, the crystal growth proceeded along TD during crystallization in the oriented state under rolling. The 020 pole of the quench rolled sheet was more sharply distributed to TD than the 200 pole did to ND, contrary to the hot rolled sheet.

The pole figures of the heavily quench rolled sheet (λ = 3.67) showed much similarity to those of the heavily hot rolled sheet (λ = 3.33) (Fig. 5) and were not shown here.

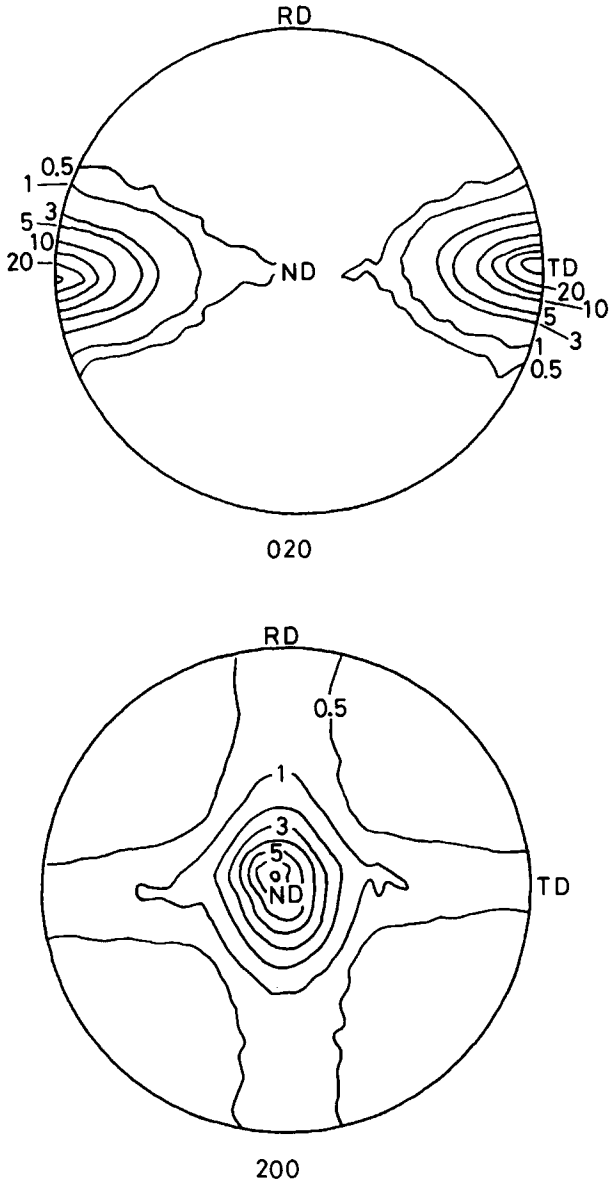

Fig. 6. WAXD pole figures of the quench rolled 240 M sheet (T_r = 100°C, λ = 1.48).

Crystallite Size

The crystallite sizes in the direction normal to the (200) and (020) planes, D_{200} and D_{020}, are shown in Figure 7. The relationship between crystallite size and draw ratio for the quench rolled sheet was analogous to that for the hot rolled sheet. The value of D_{200} monotonically decreased with increasing draw ratio, while D_{020} did not appreciably change with draw ratio.

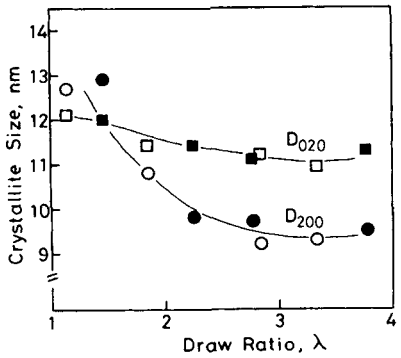

Fig. 7. Crystallite sizes vs. draw ratio (λ) relationship for 240 M sheets (T_r = 100°C): (○,□) hot rolled sheet; (●,▲) quench rolled sheet: D_{200} (○,●) and D_{020} (□,■) are the crystallite sizes in the direction normal to the (200) and (020) planes, respectively.

Small Angle X-Ray Scattering

Figure 8 shows SAXS patterns of the hot rolled sheets with incident X-ray beam parallel to ND and TD. When the X-ray beam was parallel to ND, the SAXS of the original and lightly rolled (λ = 1.14) sheets indicated ring-shaped patterns originating from randomly distributed lamellar structure in the RD–TD plane. With increasing draw ratio, the SAXS pattern changed into a two-point pattern on the meridian and the SAXS intensity decreased at a higher draw ratio (λ ≥ 2.84). The regularity in the periodic structure in the RD–TD plane was reduced in the heavily rolled sheets.

When the X-ray beam was parallel to TD, a well-defined four-point SAXS pattern was observed above λ = 1.86 and suggested a tilting of lamellae in the RD–ND plane. The angle ψ of the intensity maxima from RD corresponds to the tilting angle of lamellar normal from RD. At lower draw ratio (λ = 1.14), the four-point diagram was not clearly resolved.

The SAXS results for the quench rolled sheets had much similarity to that of the hot rolled sheets.

The chain inclination angle χ with respect to the lamellar normal and the long

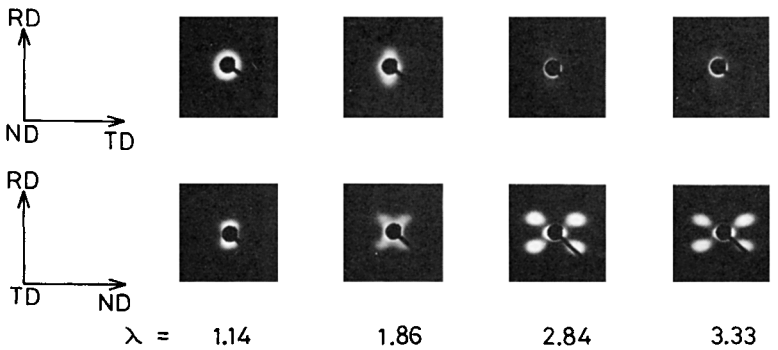

Fig. 8. SAXS patterns of hot rolled 240 M sheets (T_r = 100°C).

TABLE III
Lamellar Structural Data on Hot Rolled and Quench Rolled 240 M Sheet (T_r = 100°C)

Sample	Draw ratio λ	Long period (nm)		Lamellar inclination angle (°)		Chain inclination angle with respect to RD, θ (°)
		L[a]	l[a]	ψ[b]	χ[b]	
Hot rolled	1.14	45–		0–30	0–30	0
sheet	1.86	42–	51–	49	34	15
	2.84	20	39	58	58	0
	3.33	19	41	62	62	0
Quench rolled	1.46	41	41	0	0	0
sheet	2.25	50–	87–	55	55	0
	2.77	27–	57–	62	62	0
	3.67	18	39	63	63	0

[a] L and l are the long periods along lamellar normal and chain direction, respectively.
[b] ψ and χ are the lamellar inclination angles with respect to RD and chain direction, respectively.

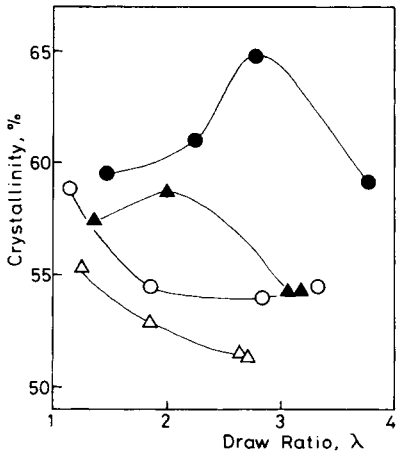

Fig. 9. Crystallinity vs. draw ratio (λ) relationship for 240 M sheets: (△) hot rolled sheet (T_r = 70°C); (○) hot rolled sheet (T_r = 100°C); (▲) quench rolled sheet (T_r = 70°C); (●) quench rolled sheet (T_r = 100°C).

period l along the chain direction are expressed as

$$\chi = \psi - \theta \tag{1}$$

$$l = L/\cos \chi \tag{2}$$

where L, ψ, and θ are the long period along lamellar normal, the lamellar inclination angle, and the chain inclination angle, respectively. The values of L, ψ, θ, χ, and l are listed in Table III. With increasing draw ratio, the angles ψ and χ increased and the long periods L and l decreased.

Crystallinity

The degrees of crystallinity of the hot rolled and the quench rolled sheets are shown in Figure 9. The degree of crystallinity of the hot rolled sheet (○,△) decreased with increasing draw ratio. The degree of crystallinity of the quench rolled sheet (●,▲) increased with increasing draw ratio in the low draw ratio range, but began to decrease in the high draw ratio range. The degree of crystallinity tended to be higher at a higher rolling temperature.

Melting Behavior

The DSC melting curves of the hot rolled and the quench rolled sheets are shown in Figure 10. By hot rolling and quench rolling, the melting peak shifted to the high temperature region. The increase in the peak melting temperature is mainly due to the effect of the strained amorphous chains.

DISCUSSION

Rolling Temperature

With increasing rolling temperature to the range of the crystalline dispersion

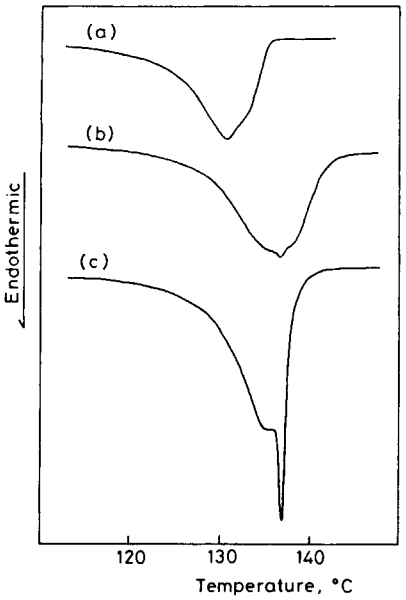

Fig. 10. DSC curves for 240 M sheets: (a) pristine sheet; (b) hot rolled sheet (T_r = 100°C, λ = 3.33); (c) quench rolled sheet (T_r = 100°C, λ = 3.67).

temperature (80–110°C) of polyethylene, drawability of the polymer is enhanced. However, as the rolling temperature approaches the melting temperature, the deformation of the sheet is dominated by the elastic motion of the amorphous chains. Therefore, the optimum temperature for the hot rolling was about 100°C.

Lattice Twinning

Hay and Keller[3] and Lewis et al.[5] studied the crystal orientation of rolled polyethylene and reported that the compressive forces generated by amorphous chains cause twinnings of lattice along the (310) and (110) planes. The 200 pole maxima caused by (310) and (110) twinnings should be located about 68° and 54° from the main maximum, respectively, in the ND–TD line.[5,6] In the heavily rolled sample (λ = 3.33), a small 200 pole maximum was observed at 57° from ND, in addition to the main maximum at ND (Fig. 5). Therefore, both (310) and (110) twinnings are considered to be produced by heavy rolling. The 020 pole figure of the heavily rolled sample can be explained in the analogous way.

Mechanism of Deformation by Hot Rolling

As rolling proceeded, the a-axis became oriented to ND, which is the direction of compression. The similar tendency was observed for the rolled sheets[3,5,6] and the extrudate[18] of NMW-HDPE. These results suggested that the deformation proceeded through the slippage along the (100) plane.

The crystallite size D_{200} decreased with increasing draw ratio up to $\lambda \sim 2$ (Fig.

7), suggesting that the cleavage of crystallites occurred along the (100) plane at the initial stage of hot rolling.

Although the value of D_{200} was almost unchanged at $\lambda > 2$, the lamellar inclination angle ψ continued to increase with increasing draw ratio. The lamellar structure would be deformed through the intercrystallite slip in the higher draw ratio range ($\lambda > 2$).

Comparison of the Quench Rolled Sheet with the Hot Rolled Sheet

At low draw ratio, there was a difference in pole figures between the hot rolled sheet and the quench rolled sheet. Although the a-axis orientation to ND was preceded to the b-axis orientation to TD in the former (Fig. 3), the b-axis of the latter was more highly oriented to TD than the a-axis was to ND (Fig. 6). This is because the b-axis was well oriented to the direction of crystal growth, TD during the course of quench rolling.

On the other hand, at high draw ratio ($\lambda \leq 2.7$), the quench rolled sheet showed much similarity to the hot rolled sheet in SAXS pattern, pole figure, and crystallite size. This suggests that the quench rolling to high draw ratio consists of the crystallization in the oriented state at the initial stage and the succeeding plastic deformation of the crystallized texture.

Comparison with the Hot Rolling of NMW-HDPE

Owing to the presence of the network superstructure generated by the entanglements of long molecular chains,[19] UHMW-PE loses the fluidity and shows rubberlike elasticity. As the shape of the molten UHMW-PE sheet is stable at 140–150°C, UHMW-PE can be quench rolled from the molten sheet.

Smith et al. have reported that the presence of the entanglements reduces the drawability of the polymer sheet.[20] The maximum draw ratio obtained in this work was 3–4 and smaller than that for NMW-HDPE.[6]

There are distinct differences between hot rolled NMW-HDPE sheets and hot rolled UHMW-PE sheets in lamellar structure. The SAXS data of hot rolled NMW-HDPE revealed the presence of two kinds of lamellar structure,[6] one in which inclined lamellae give a four-point SAXS diagram and another in which lamellar normals are oriented to RD. With increasing draw ratio, the inclination angle of the inclined lamellae decreased as the c-axis became aligned to RD. On the other hand, hot rolled UHMW-PE showed a four-point SAXS pattern on the diagonal above $\lambda = 1.86$, suggesting that hot rolled UHMW-PE contains only inclined lamellae. In contrast to the hot rolled NMW-HDPE, the lamellar inclination angle of hot rolled UHMW-PE increased with draw ratio independently of the chain orientation.

CONCLUSION

By hot rolling and quench rolling of UHMW-PE, the a-, b-, and c-axes tended to be oriented to ND, TD, and RD, respectively. In the heavily rolled sample, (310) and (110) lattice twinnings were observed.

The SAXS investigation revealed the presence of inclined lamellar structure in the RD–ND plane. In contrast to the hot rolled NMW-HDPE sheet, the la-

mellar inclination angle of the rolled UHMW-PE sheet increased with increasing draw ratio.

The dominant mechanism of deformation is the slippage along the (100) plane in the chain direction. At low draw ratio ($\lambda < 2$), partial breakup of crystallites along the (100) plane was observed.

References

1. S. Bahadur and A. Henkin, *Polym. Eng. Sci.*, **13**, 422 (1973).
2. V. J. Dhingra, J. E. Spruiell, and E. S. Clark, *Polym. Eng. Sci.*, **21**, 1063 (1981).
3. I. L. Hay and A. Keller, *J. Mater. Sci.*, **1**, 41 (1966).
4. D. M. Gezovich and P. H. Geil, *J. Mater. Sci.*, **6**, 509 (1971).
5. D. Lewis, E. J. Wheeler, W. F. Wheeler, W. F. Maddams, and J. E. Preedy, *J. Polym. Sci., A-2*, **10**, 369 (1972).
6. O. Yoda and I. Kuriyama, *J. Polym. Sci., Polym. Phys. Ed.*, **15**, 733 (1977).
7. K. Nakayama, H. Tamamura, H. Asazawa, and H. Kanetsuna, *J. Jpn. Soc. Tech. Plasticity*, **21**, 1096 (1980).
8. I. L. Hay and A. Keller, *J. Mater. Sci.*, **2**, 538 (1967).
9. T. T. Wang, H. S. Chen, and T. K. Kwei, *Polym. Lett.*, **8**, 505 (1970).
10. T. K. Kwei, T. T. Wang, and H. E. Bair, *J. Polym. Sci., C*, **31** 87 (1970).
11. M. Takiura and M. Ishida, *Plastics*, **25**(4), 77 (1974).
12. T. Shiraki, *Plastics*, **28**(5), 57 (1977).
13. G. Meinel and A. Peterlin, *Kolloid Z. Z. Polym.*, **242**, 1151 (1970).
14. K. S. Han, J. F. Wallace, R. S. Truss, and P. H. Geil, *J. Macromol. Sci. Phys.*, **B19**, 313 (1981).
15. P. Scherrer, *Gött. Nachr.*, **2**, 98 (1918).
16. P. R. Swan, *J. Poly. Sci.*, **56**, 403 (1962).
17. M. G. Gubler and A. J. Kovacs, *J. Polym. Sci.*, **34**, 551 (1959).
18. K. Imada, T. Yamamoto, K. Shigematsu, and M. Takayanagi, *J. Mater. Sci.*, **6**, 537 (1971).
19. J. Steidel and Z. Pelzbauer, *J. Polym. Sci., C*, **38**, 345 (1972).
20. P. Smith, P. J. Lemstra, and H. C. Booij, *J. Polym. Sci., Polym. Phys. Ed.*, **19**, 877 (1981).

Received September 20, 1982
Accepted October 29, 1982